URBAN SPATIAL AND TEMPORAL CHANGES ANALYSIS BASED ON SPECTRAL, POLARIMETRIC, TEMPORAL, SPATIAL DIMENSIONS AND DECISION LEVEL FUSION

Pei Liu[1], Peijun Du[1, 2], Paolo Gamba[3]

1. China University of Mining and Technology, Key Laboratory for land environment and disaster monitoring of SBSM, Xuzhou, China; email: cumtlp@gmail.com
2. Nanjing University, Department of Geographical Information Sciences, Nanjing, China; e-mail: dupjrs@126.com
3. Dipartimento di Elettronica, Univ. di Pavia, Pavia, Italy; e-mail: paolo.gamba@unipv.it

ABSTRACT

In order to monitor the pattern, distribution and trend of urban land use/ land cover change, it is necessary to integrate polarization, spatial, spectral and multi-temporal remotely sensed data to assess the spatial pattern and dynamics changes of urban areas in both the spatial and the temporal dimensions. In this paper, multi-temporal Landsat TM/ETM+ optical data, and dual-polarized, horizontal-horizontal (HH) and vertical-vertical (VV) PALSAR data are integrated. Specifically, derive spatial information is included by means of eight textures extracted from PALSAR HH and HV data, and from optical bands using Grey-level Co-occurrence Matrix (GLCM), including the mean, variance, homogeneity, contrast, dissimilarity, entropy, second moment, and correlation. They are used to generate multi-temporal land cover maps by image classification and decision level fusion. Finally, more than ten quantitative landscape indices, including Number of Patches (NP), Patch Density (PD), Largest Patch Index (LPI), Mean of patch Area Distribution (AREA_MN), Area-weight-mean of Shape index (SHAPE_AM), Area-weight-mean of Fractal dimension index (FRAC_AM), Area-weight-mean of Euclidean Nearest-Neighbor Distance (ENN_AM), Contagion Index (CONTAG), Interspersion and Juxtaposition Index (IJI) and Shannon's Diversity Index (SHDI), are selected to analyse and evaluate the spatial-temporal changes at the patch level, class level and landscape level. At the same time, land use and land cover transfer matrixes are used to assess the dynamic change trends for different land cover types. The results demonstrate the significance of combining multi-temporal optical data, SAR data and spatial information by means of texture variables for landscape pattern monitoring. Analysis based on Land Use and Land Cover (LULC) and landscape indexes at the annual and seasonal levels show LULC changes between 2001 and 2011 and allow detection exactly in what season they happened.

INTRODUCTION

With the development of the urbanization process, land covers and landscape patterns are seriously affected by human activities. Remotely sensed data and techniques, undoubtedly, are the most powerful way and information source to monitor, analyse and model landscape and its changes in urban areas. Many international researchers have worked on this line of research [1-6]. With an increasing number of satellite sensors are able to record data over the same scene, one trend still to be fully evaluated is how to make use or integrate all the multi-source data information, such as polarizations, spatial dimensions, temporal and spectral patterns, for landscape mapping, analysing and change trend evaluating [7].

The purpose of this study is to analyse and evaluate the land use/cover changes (LULC) status and trend with respect to both their spatial and temporal aspects, based on the landscape pattern indexes achieved by integrating polarization, spatial, spectral and temporal information from optical and dual-polarized SAR data. The idea is to obtain landscape pattern results using multi-source

information fusion and then analyze and evaluate LULC change by means of the transfer matrix and landscape indexes at the class and landscape levels.

METHODS

An exurb mining area with subsidence problems caused by mining activity is selected as test site, covering the area from $33^0$43'N to $34^0$58'N and from $116^0$22'E to $118^0$40'E. Multi-temporal Landsat optical and PALSAR data recorded on January 27, 2009, April 8, 2009, May 3, 2009, August 31, 2009, November 3, 2009, April 3, 2001, May 11,2003, April 14, 2005, May 4, 2007, March 30, 2011, May 8, 2008 and June 26, 2009 are used, together with two vector maps. These data are grouped into two datasets as shown in Table 1.

Table 1. Dataset selected by seasonal and annually

	Quarterly				Annually					
	Spring	Summer	Fall	Winter	2001	2003	2005	2007	2009	2011
Optical	1(4).27(8).09	05.03.09	08.31.09	11.03.09	04.03.01	05.11.03	04.14.05	05.14.07	05.03.09	03.30.11
SAR	05.08.2008									

The Landsat 7 data obtained on April 14, 2005 and March 30, 2011 are affected by problems due to scans line corrector (SLC) turned off. These data are scan gap filled using the local linear histogram matching technique [8]. Moreover, the January 27, 2009 Landsat data do not cover the whole research area and thus are mosaicked with adjacent track data obtained three months later, on April 8. Dual-polarization ALOS PALSAR raw data are processed into multi-look intensity (MLI) images first, with 2 range looks and 4 azimuth looks. Then, terrain correction is applied using SRTM 90m Digital Elevation Data (DEM). Following the DEM geocoding procedure, SAR data are resampled to a grid with pixel spacing equal to the one in the optical images. Finally, a Gamma-Map despeckle filter is selected to mitigate speckle, while preserving texture. For both the optical and SAR data sets, spatial texture information are created using the Grey-Level Co-occurrence Matrix (GLCM) method. By using a number of these features, image stacks including different data sets according to possible processing strategies are shown in Table 2.

Table 2. Spatial and spectral features combination strategies

Data source.	Numbers of variables	Combinations
SAR	18	HH/HV SAR and corresponding GLCM textures (PALSAR and PALSAR textures)
Optical	45/54/63/72	Optical and GLCM textures (TM/ETM+, textures for 5/6/7/8 bands)
SAR + Optical. 04.03.2011	72	HH/HV SAR, Optical, GLCM textures for Landsat and SAR.
SAR + Optical. 04.11.2003	63	HH/HV SAR, Optical, GLCM textures for Landsat and SAR
SAR + Optical. 04.14.2005	63	HH/HV SAR, Optical, GLCM textures for Landsat and SAR
SAR + Optical. 05.14.2007	81	HH/HV SAR, Optical, GLCM textures for Landsat and SAR
SAR + Optical. 05.03.2009	81	HH/HV SAR, Optical, GLCM textures for Landsat and SAR
SAR + Optical. 03.30.2011	45	HH /HV SAR, Optical, GLCM textures for Landsat and SAR
SAR + Optical.01.27.2009	81	HH/HV SAR, Optical, GLCM textures for Landsat and SAR
SAR + Optical.08.31.2009	90	HH/HV SAR, Optical, GLCM textures for Landsat and SAR
SAR + Optical.11.03.2009	90	HH/HV SAR, Optical, GLCM textures for Landsat and SAR

In order to analyze the scenes, three land cover classes, namely building, water and others are considered, where the last class includes for the vast majority of cases vegetated areas. These classes are extracted from both optical and SAR data, and their selection is based on the need to monitor LULC in a real situation with focus on fast spreading urbanization processes. A Support Vector Machine (SVM) supervised classifier is adopted to extract land cover maps, because of its superior classification performances with respect to other classifiers in terms of efficiency, accuracy and generalization of the results [9].

The LULC maps at one date and temporal trends are combined exploiting these multi-temporal classification maps. Landscape patterns and trends are qualitatively and quantitatively analysed and evaluated using land use/land cover transfer matrix and landscape indexes at both the class and landscape levels. The flow chart of this work is shown in Figure 1.

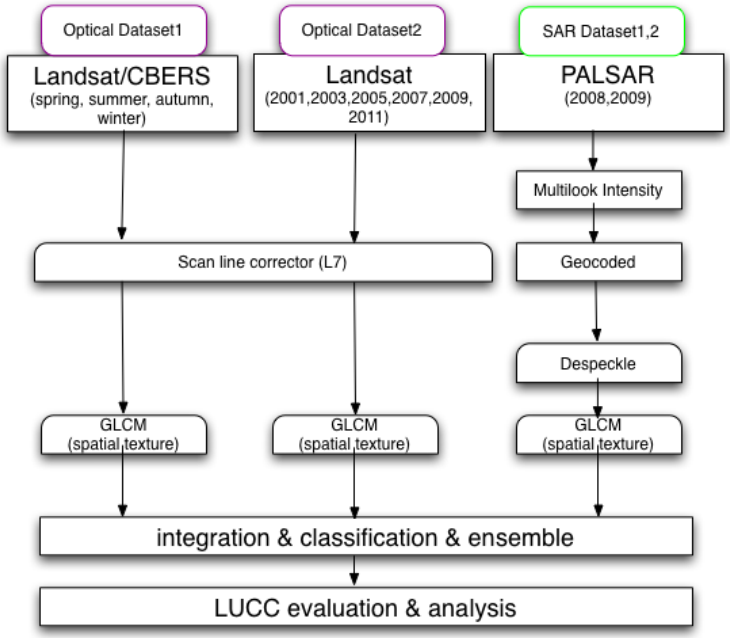

Figure 1. Flow chart of adopted method in this paper.

RESULTS

The experimental results of this research come from the analysis of multi-temporal scenes of Landsat TM/ETM+ optical data obtained among 2001 to 2011 and ALOS dual-polarization PALSAR data acquired on May 5, 2008. The research area is depicting a portion of the exurb mining area of Xuzhou, in Jiangsu province, P. R. China. Both annual changes during a 20 year span and a special seasonal change trend in 2009 are considered and analysed according to the above mentioned classification approach. The best land cover maps obtained by means of an SVM classifier and optical and SAR spectral and spatial feature combinations are used for change detection. One example is shown for April 14, 2007 in Figure 2, together with the corresponding ground truth, while the overall accuracy for various input data and feature combinations are shown in Table 3. The results shown clearly that the ability to combine spatial and spectral information from both SAR and optical images increases the mapping accuracy. Indeed, the overall accuracy of final result has an increase of 20% and 2% with respect to land cover maps obtained using only SAR or optical data, respectively.

After classifying the available multi-temporal data sets, landscape pattern trends are analysed using transfer matrix and shown in Figure 4. The annually LULC trend chart demonstrates that during the twenty years from 2001 to 2011 the water body land cover area has been stable; the primarily LULC changing categories are building area and others; during the periods from 2003 to

2006 and from 2009 to 2011 the change is from building to others, while from 2006 to 2009 is from the others category to building area. A temporally finer trend for the LULC change using quarter data sets and thus extracting a seasonal transfer matrix is shown in the right part of Figure 3. It demonstrates both the transform trend from building area to others from 2009 to 2012 and the fact that it started exactly since the summer of 2009.

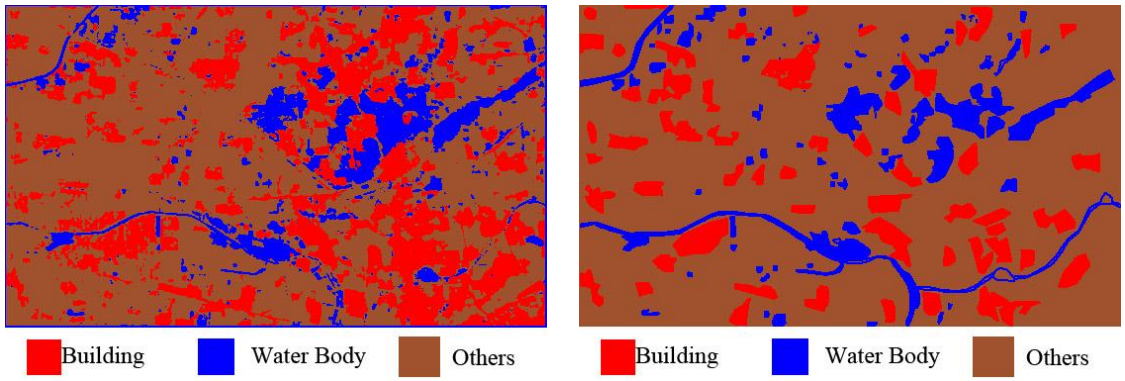

Figure 2. (a) Ensemble result of TM optical and SAR using majority algorithm for the test area (exurb mining area around XuZhou, P.R. China); (b) corresponding ground truth.

Table 3. Overall accuracy of the classification result

%	SAR_HH	SAR_HV	Majority	2001	2003	2005	2007	09.01	09.05	09.08	09.11	2011
OA	51.3	54.02	74.92	67.62	67.62	73.18	74.92	63.61	61,97	70.81	72.04	69.74

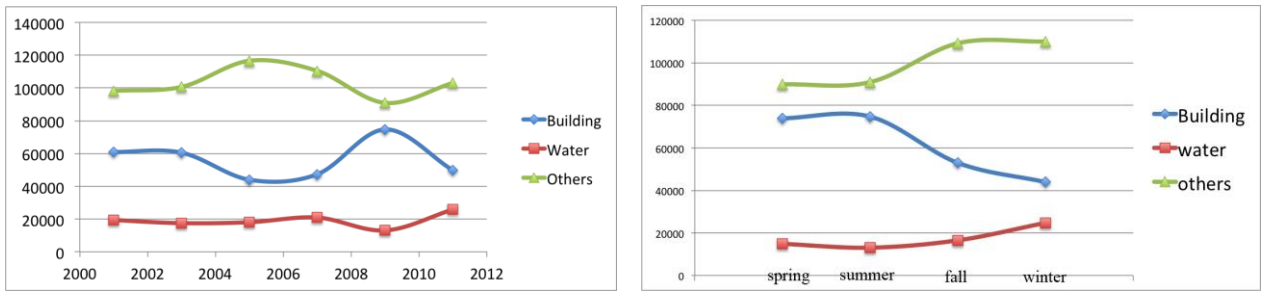

Figure 3. LULC trend calculated based on transfer matrix.

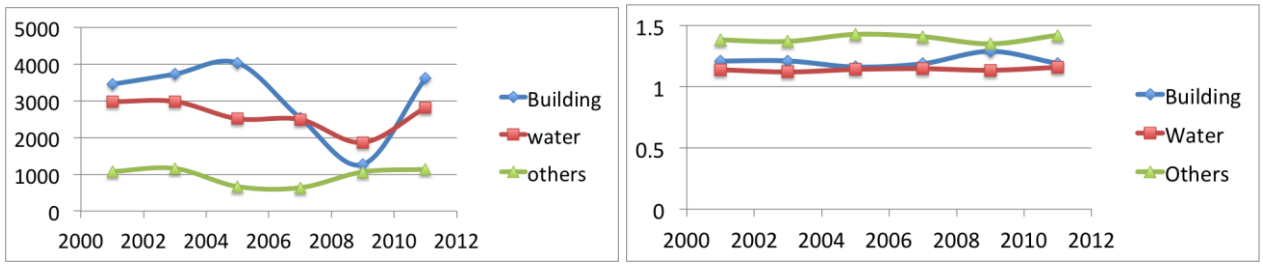

(a) NP (b) FRAC_AM

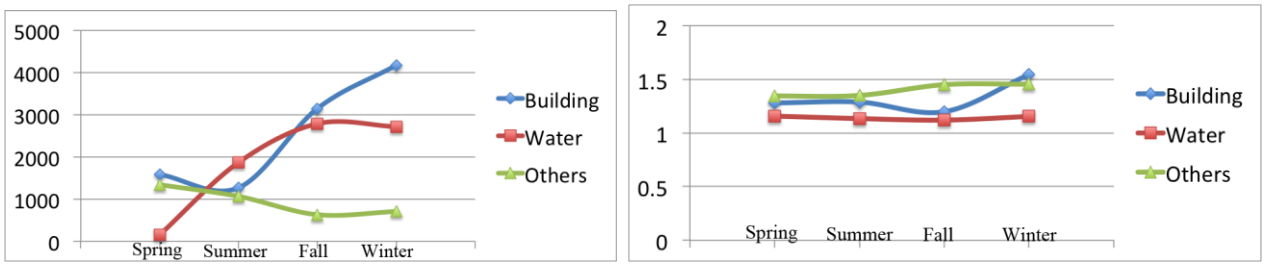

(c) NP (d) FRAC_AM

Figure 4. LULC analysis at the class level using landscape indexes.

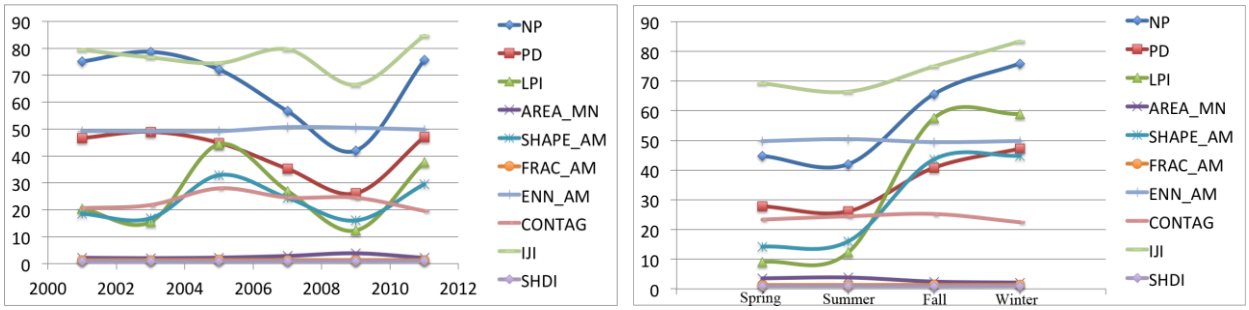

Figure 5. Finer temporal LULC analysis at the landscape level on the basis of landscape indexes.

From the analysis based on landscape indexes at the class level, we can conclude that the NP of building area fluctuated, decreases gradually from 2005 to 2009 and increases from 2009 to 2011; the NP of water body and others seem instead relatively stable. In the seasonal trends map, NP of the others category seems stable, while the NP of building area increases gradually and NP of water body increases from summer to fall and decreases from fall to winter. This effect may have been caused by rainfalls, as the area follows the temperate continental climate pattern. The NP of building areas increases as the landscape fragmentation become more and more serious. FRAC_AM is used to measure complexity of the landscape patch shapes. From the changes of FRAC_AM values in both the annual and seasonal charts, its is possible to note that the complexity of landscape patch shapes increases from 1.16 to 1.28 in building areas and from 1.38 to 1.42, while the class with fewest changes is the water body, from 1.12 to 1.15.

The analysis at the landscape level shows that the trend of NP and PD is consistent because they indicate the degree of landscape fragmentation; LPI display as irregularity wave fluctuations in the annual chart and as gradually increase trends in the seasonal chart; IJI value displays as a horizontal line before 2007 and then as a decrease and increase trend from 2007 to 2009 and from 2009 to 2011 in the annual map. In the seasonal map this value has a increase trend from summer to winter. The lowest values of NP and PD appear in 2009, which means that the lowest crushing landscape status was achieved in that year. IJI value shows the overall spread and tie state among different landscapes, whose lowest value once more appears in 2009, meaning that there is a smallest mutual neighbor probability in 2009 of this research area than any other year. Finally, according to the analysis from seasonal changes of the index, we can see that the smallest mutual neighbor probability happened in the summer of that year.

CONCLUSIONS

The results reported in this paper show that it is feasible to merge polarization, spectral, temporal and spatial information for land use/ cover change detection and analysis. The results in this experiment confirm that the best mapping results is achieved by a mix of optical data, optical texture, SAR data and SAR textures, but more analyses are required to understand better which combination works best in many different situations.

As for the temporal trends obtained from the analysis of the multi-annual and season LULC maps, change monitoring based on transfer matrix and landscape indexes shows that there were dramatic changes in 2005 and especially in 2009. A temporally finer at the seasonal level shows that the change in 2009 happened in the summer of that year.

ACKNOWLEDGEMENTS

The Chinese authors acknowledge the Opening Foundation of The Key Laboratory of Mapping from Space of State Bureau of Surveying and Mapping (Grant No. K201007), and the graduate students research and Innovation Plan of Jiangsu (CX09B_115Z). All authors are grateful to the

Dragon 2 Program Project 5317, sponsored by the Ministry of Science and Technology of China and the European Space Agency.

REFERENCES

1. Hao, H.-m. and Z.-y. Ren, *Land Use/Land Cover Change (LUCC) and Eco-Environment Response to LUCC in Farming-Pastoral Zone, China.* Agricultural Sciences in China, 2009. **8**(1): p. 91-97.
2. Schweitzer, C., J.A. Priess, and S. Das, *A generic framework for land-use modelling.* Environmental Modelling & Software, 2011. **26**(8): p. 1052-1055.
3. Yu, W.H., et al., *Analyzing and modeling land use land cover change (LUCC) in the Daqing City, China.* Applied Geography, 2011. **31**(2): p. 600-608.
4. Zhan, C.S., et al., *LUCC and its impact on run-off yield in the Bai River catchment-upstream of the Miyun Reservoir basin.* Journal of Plant Ecology-Uk, 2011. **4**(1-2): p. 61-66.
5. Wang, Y.C. and C.C. Feng, *Patterns and trends in land-use land-cover change research explored using self-organizing map.* International Journal of Remote Sensing, 2011. **32**(13): p. 3765-3790.
6. Li, Y.R., H.L. Long, and Y.S. Liu, *Industrial development and land use/cover change and their effects on local environment: a case study of Changshu in eastern coastal China.* Frontiers of Environmental Science & Engineering in China, 2010. **4**(4): p. 438-448.
7. Schweitzer, C., J.A. Priess, and S. Das, *A generic framework for land-use modelling.* Environmental Modelling & Software, 2011. **26**(8): p. 1052-1055.
8. Scaramuzza, P., et al., SLC Gap-Filled Products Phase One Methodology. http://vip-136-10.cr.usgs.gov/documents/SLC_Gap_Fill_Methodology.pdf
9. Giacco, F., et al., *Uncertainty Analysis for the Classification of Multispectral Satellite Images Using SVMs and SOMs.* Ieee Transactions on Geoscience and Remote Sensing, 2010. **48**(10): p. 3769-3779.